



PERGAMON

Available online at [www.sciencedirect.com](http://www.sciencedirect.com)

SCIENCE @ DIRECT®

International Journal of  
**HEAT and MASS  
TRANSFER**

International Journal of Heat and Mass Transfer xxx (2003) xxx–xxx

[www.elsevier.com/locate/ijhmt](http://www.elsevier.com/locate/ijhmt)

## 2 Natural convective heat transfer from isothermal cuboids

3 Ewa Radziemska, Witold M. Lewandowski \*

4 Department of Apparatus and Chemical Machinery, Gdansk University of Technology ul. G. Narutowicza 11/12, 80-952 Gdańsk, Poland

### 5 Abstract

6 The paper presents results of theoretical and experimental investigations of the convective heat transfer from iso-  
7 thermal cuboid. The analytical solution was performed taking into account complete boundary layer length and the  
8 manner of its propagation around isothermal cuboid. It arises at horizontal bottom surface and grows on vertical  
9 lateral surface of the block. After changing its direction, the boundary layer occurs above horizontal surface faced up  
10 and next it is transformed into buoyant convective plume. To verify obtained theoretical solution the experimental  
11 study has been performed. The experiment was carried out for three possible positions of tested the same cuboid.

12 As the characteristic linear dimension in Nusselt–Rayleigh theoretical and experimental correlations we proposed  
13 the ratio of six volumes to the cuboids surface area, for the analogy to the same ratio using as the characteristic di-  
14 mension for the sphere, which is equal to the sphere's diameter. It allowed performing the experimental results inde-  
15 pendently from the orientation of the block. The Rayleigh numbers based on this characteristic length ranged from  $10^5$   
16 to  $10^7$ . The Nusselt number describing intensity of convective heat transfer from the cuboid can be expressed by:  
17  $Nu = XRa^{1/5} + YRa^{1/4}$ , where  $X$  and  $Y$  are coefficients dependent on the cuboid's dimensions. For the range of provided  
18 experiment the experimental Nusselt–Rayleigh relation can be presented in the form:

$$Nu = 1.61Ra^{1/5} \text{ or } 0.807Ra^{1/4}$$

20 with the good agreement with the theoretical one recalculated for the tested cuboid dimensions.

21 © 2002 Published by Elsevier Science Ltd.

### 23 1. Introduction

24 Free convective heat transfer, especially from bodies  
25 or objects limited by cuboids surfaces, take place in  
26 building engineering, central heating, electronics,  
27 aeronautics, aquanauts, chemical apparatus, lighting  
28 industry. In these branches cubes are very often used as  
29 insulating, constructing or shielding surfaces.

30 The mechanism of heat transfer considered from all  
31 surfaces of cuboid is more complicated than from flat  
32 horizontal or vertical plates treated separately. The  
33 boundary layer from downward faced bottom of the  
34 cuboid has the significant influence on the formation of

boundary layer on vertical side and next on boundary 35  
layer above horizontal top of the block. Up to now these 36  
configurations of surfaces (horizontal flat plates facing 37  
downward [1–4], horizontal flat plates facing upward [5– 38  
11] and vertical plates [1,9,12]) have been studied theo- 39  
retically and experimentally independently. In the case 40  
of cuboids we found significantly less papers devoted 41  
them. Culham et al. [13] proposed three analytical 42  
models presented for determining laminar and forced 43  
convection heat transfer from isothermal cuboids. It is a 44  
convenient method for calculating an average Nusselt 45  
number, base on cuboid dimensions, thermophysical 46  
properties and the approach velocity. Cha and Cha [14] 47  
presented the numerical and experimental investigations 48  
results of 3D natural convection flows around two in- 49  
teracting isothermal cubes. Yovanovich [15] compared 50  
models of Chamberlain, Stretton and Clemes for cube 51  
and cuboid and also Karagiosis and Saunders model for 52  
vertical plate in microelectronic heat sink applications. 53  
Meinders et al. [16] provided experiments of the local 54

\* Corresponding author. Tel.: +48-58-347-24-10/18-74; fax:  
+48-58-347-24-58/18-74.

E-mail address: [ewarad@chem.pg.gda.pl](mailto:ewarad@chem.pg.gda.pl) (W.M. Lewandow-  
ski).

### Nomenclature

$a = \frac{\lambda}{c_p \rho}$	thermal diffusivity (m <sup>2</sup> /s)
$a$	width of the cuboid (m)
$A$	control surface across the boundary layer (m <sup>2</sup> )
$b$	length of the cuboid (m)
$c$	height of the cuboid (m)
$C$	$Nu(Ra)$ relation constant (–) (Eq. (33))
$c_p$	specific heat at constant pressure (J/(kg K))
$dS$	control surface of heated surface (m <sup>2</sup> )
$F$	surface of the cuboid (m <sup>2</sup> )
$g$	acceleration due to gravity (m/s <sup>2</sup> )
$i$	enthalpy (J/kg)
$I$	electric current (A)
$L$	characteristic length (m)
$n$	$Nu(Ra)$ relation exponent (–) (Eq. (33))
$Nu = \frac{qL}{\lambda}$	Nusselt number (–)
$Pr = \nu/a$	Prandtl number (–)
$\dot{Q}$	heat flux (W)
$Ra = \frac{g\beta\Delta T L^3}{\nu a}$	Rayleigh number (–)
$T$	temperature (°C or K)
$\Delta T$	temperature difference (K)
$U$	voltage (V)
$V$	volume of the cube (m <sup>3</sup> )
$w$	velocity of the fluid (m/s)
$x'$	the boundary layer length measured along the streamlines in the bottom corner region (m)

### Greek symbols

$\alpha$	heat transfer coefficient (W/(m <sup>2</sup> K))
$\beta$	average volumetric thermal expansion coefficient (1/K)
$\delta^*$	dimensionless boundary layer thickness (–)
$\delta$	boundary layer thickness (m)
$\delta_f$	final thickness of dimensionless boundary layer (m)
$\lambda$	thermal conductivity of the fluid (W/m K)
$\nu$	kinematic viscosity of the fluid (m <sup>2</sup> /s)
$\Theta$	dimensionless temperature defined by Eq. (4)

### Subscripts

1l	region 1 lateral
1c	region 1 corner
2l	region 2 lateral
2c	region 2 corner
3l	region 3 lateral
3c	region 3 corner
c	convective
f	final
n	normal
r	radiative
$\tau$	tangential
w	wall
$\infty$	bulk fluid

55 convective heat transfer from a wall-mounted single  
56 array of cubical protrusions along a wall at a wind  
57 tunnel. Nakamura et al. [17] presented the data about  
58 the cooling design of electric equipment in the form of  
59 cubes and square blocks. Culham and Yovanovich with  
60 Lee [18] calculated the thermal performance of several  
61 heat sinks using a flat plate boundary model, also for  
62 isothermal cuboids with the square root of the surface  
63  $A^{1/2}$  as the characteristic length in the form:

64  $Nu_{\sqrt{A}} = 3.42 + 0.524Ra_{\sqrt{A}}^{1/4}$  for cuboids with aspect  
65 ratios length/width = 1:1 and  $Nu_{\sqrt{A}} = 3.89 + 0.594Ra_{\sqrt{A}}^{1/4}$   
66 for cuboids with aspect ratios length/width = 10:1.

7 This paper is focused on analytical solution of sim-  
8 plified Navier–Stokes and Fourier–Kirchhoff equations,  
9 described natural convective heat transfer from iso-  
0 thermal cuboids immersed in fluid treated as unlimited  
1 space.

2 Obtained for cuboids of different shapes (determined  
3 by length, width and height) solution has been verified  
4 experimentally. In the experimental study we tested the  
5 same cuboid with dimensions 0.2 m × 0.1 m × 0.045 m  
6 situated in three positions: vertical I, lateral II and

horizontal III. In this way the errors of measurements 77  
were for all tested positions the same. 78

## 2. The theoretical considerations 79

80 According to the surface orientation to the gravita-  
81 tional acceleration the cuboid was divided into three  
82 regions correlated with the heat transfer direction (Fig.  
83 1). Region 1 is the bottom of the cuboid and it is treated  
84 as the sum of two rectangular horizontal and faced  
85 down rectangles (1l) with the surface  $((b-a)a/2)$  each  
86 and eight horizontal down-faced triangles (1c) with the  
87 surface  $(a^2/8)$  each. Region 2 is composed of two ver-  
88 tical rectangles (2l) with the surface  $((b-a)c)$  each and  
89 eight vertical rectangles (2c) with the surface  $(ac/2)$  each.  
90 Region 3 is the rectangular horizontal plate facing up-  
91 ward, created by two rectangles (3l) with the surface  
92  $((b-a)a/2)$  each and eight triangles (3c) with the sur-  
93 face  $(a^2/8)$  each.

94 The mean heat transfer coefficient for the cuboid can  
95 be obtained from the energy balance ( $Q = Q_1 + Q_2 + Q_3$ )

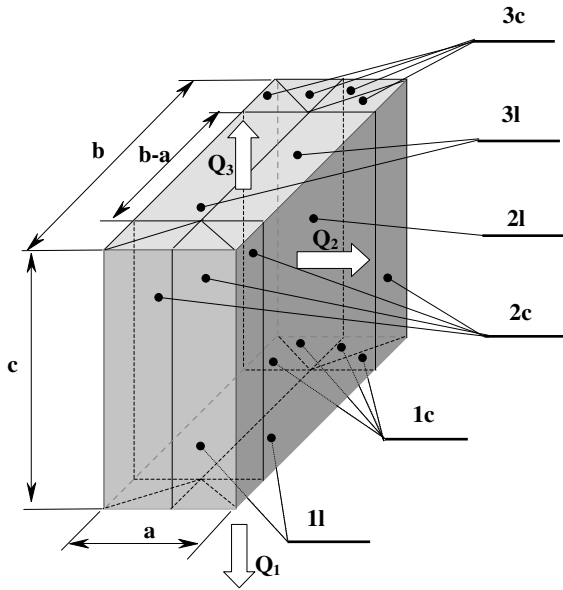


Fig. 1. The regions of the cuboid, correlated with the heat transfer phenomenon: 1—horizontal faced-down, 2—vertical, 3—horizontal faced up and subregions: 1—lateral, c—corner.

96 by averaging heat transfer coefficients obtained for all  
97 mentioned above regions and subregions:

$$\bar{\alpha} = \frac{(b-a)a(\bar{\alpha}_{1l} + \bar{\alpha}_{3l}) + a^2(\bar{\alpha}_{1c} + \bar{\alpha}_{3c}) + 4ac\bar{\alpha}_{2c} + 2(b-a)c\bar{\alpha}_{2l}}{2(ac + ab + bc)} \quad (1)$$

99 Introducing the simplifying assumptions typical for  
100 the natural convection and proposed physical model  
101 such as:

- 102 – fluid is incompressible and its flow is laminar and steady,
- 103
- 104 – the flow is predominantly parallel to the control surface of heated wall, with the boundary layer develop
- 105 with the distance along the surface,
- 106
- 107 – physical properties of the fluid in the boundary layer and in the undisturbed region are constant,
- 108
- 109 – temperature of the cuboid's surface ( $T_w$ ) is constant,
- 110 – inertia terms, viscous dissipation and internal heat sources are neglected,
- 111
- conductive heat losses through suspension of the cuboid to the fluid is disregard in comparison with convective one,
- 13
- 14 – thickness of thermal and hydraulic boundary layers are the same
- 16

so the Navier–Stokes equations for the control space inside the boundary layer may be written for any positions of heated surface in terms:

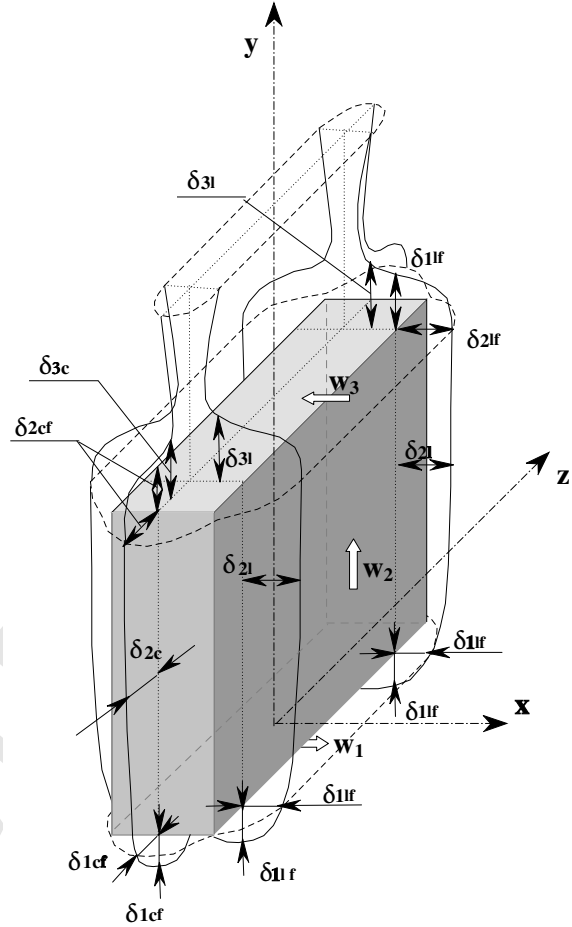


Fig. 2. The boundary layer shapes and thickness in the defined regions.

$$v \frac{\partial^2 w_\tau}{\partial n^2} + g\beta(T_\tau - T_\infty) \sin \phi - \frac{1}{\rho} \frac{\partial p}{\partial \tau} = 0 \quad (2)$$

$$g\beta(T_\tau - T_\infty) \cos \phi - \frac{1}{\rho} \frac{\partial p}{\partial n} = 0 \quad (3)$$

where ( $\phi$ ) is an angle of inclination of considered surface: ( $\phi = 0$ ) for the horizontal and ( $\phi = \pi/2$ ) for vertical surface, ( $\tau$ ) and ( $n$ ) are the tangential and normal to the fluid flow directions.

Instead of the direct form of the Fourier–Kirchhoff equation it was decided, according to Squire and Eckert [19,20], to make assumption that the temperature profile in the boundary layer is described by:

$$\Theta = \frac{T - T_\infty}{T_w - T_\infty} = \left(1 - \frac{n}{\delta}\right)^2 \quad (4)$$

132 The quasi-analytical solution of Eqs. (1)–(3), pre-  
133 sented in Ref. [21] in the form of the local and mean  
134 velocity in control space across the boundary layer are:

$$w_\tau = \frac{g\beta\Delta T}{\nu} \left[ \frac{d\delta}{d\tau} \left( \frac{n^4}{12\delta^2} - \frac{2n^5}{60\delta^3} - \frac{n^2}{6} + \frac{7\delta n}{60} \right) \cos \phi + \left( -\frac{n^2}{2} + \frac{n^3}{3\delta} - \frac{n^4}{12\delta^2} + \frac{\delta n}{4} \right) \sin \phi \right], \quad (5)$$

$$\bar{w}_\tau = \frac{1}{\delta} \int_0^\delta w_\tau dy = \frac{g\beta\Delta T\delta^2}{\nu} \left( \frac{d\delta \cos \phi}{72} + \frac{\sin \phi}{40} \right) \quad (6)$$

137 The change in mass flow intensity in control surface  
138 across the boundary layer ( $A$ ) is

$$dm = d(A\bar{w}_\tau\rho) \quad (7)$$

140 The amount of the heat necessary to create this  
141 change in mass flux is

$$dQ = \Delta i dm = \rho c_p (\bar{T} - \bar{T}_\infty) d(A\bar{w}_\tau) \quad (8)$$

143 Substitution of the mean value of the temperature

$$(\bar{T} - \bar{T}_\infty) = \frac{1}{\delta} \int_0^\delta \Delta T \left(1 - \frac{n}{\delta}\right)^2 dn = \frac{\Delta T}{3} \quad (9)$$

gives 145

$$dQ = \frac{\rho c_p \Delta T d(A\bar{w}_\tau)}{3} \quad (10)$$

The heat flux described by Eq. (9) may be compared  
to the heat flux determined by Newton's Eq. (10): 147 148

$$dQ = \alpha \Delta T dS = -\lambda \left( \frac{\partial \Theta}{\partial n} \right)_{n=0} \Delta T dS, \quad (11)$$

where ( $dS$ ) is the control surface of the heating surface. 150

From simplifying assumption of the temperature  
profile inside the boundary layer (4), the dimensionless  
temperature gradient on the heated surface may be  
evaluated as: 151 152 153 154

$$\alpha = \lambda \left( \frac{\partial \Theta}{\partial n} \right)_{n=0} = -\frac{2\lambda}{\delta} \quad (12)$$

Comparing the heat flux emitted by the wall surface  
with the heat flux transported by the fluid one can obtain: 156 157

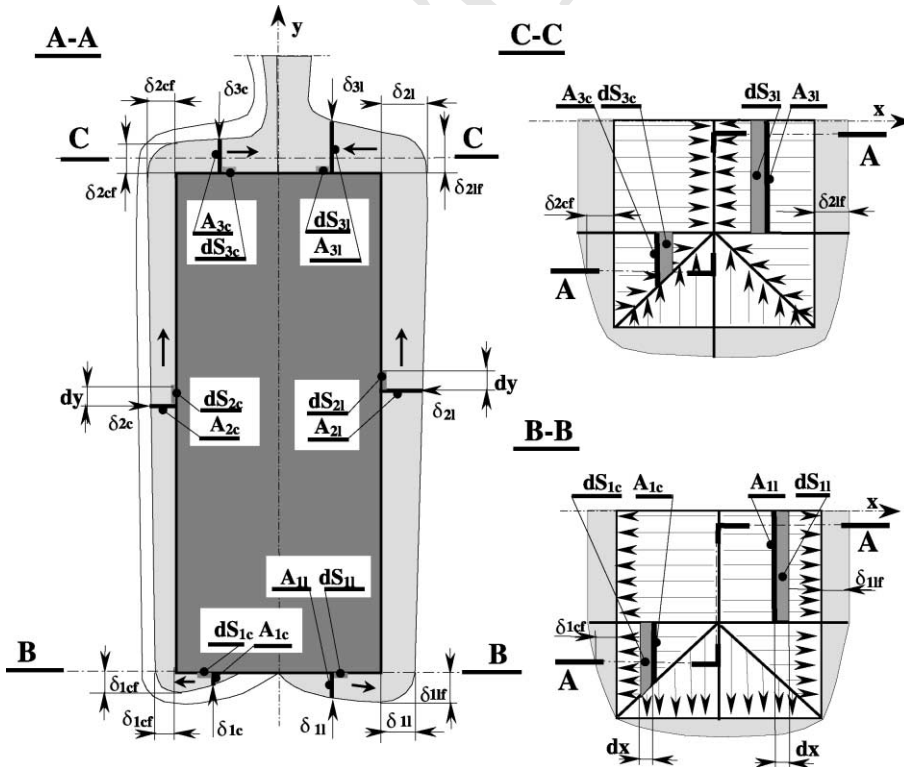


Fig. 3. Three sections of tested cuboids with boundary layers: A-A—longitudinal offset section, where the left section was made through the corner subregions, the right section -through the lateral ones; B-B—cross-section through boundary layer below down faced surface of the bottom with stream lines patterns; C-C—cross-section through boundary layer above up faced surface of the top of the cuboid with stream lines patterns.

$$\frac{1}{6} \frac{\rho c_p \delta}{\lambda} d(A \bar{w}_\tau) = dS \quad (13)$$

### 159 2.1. Detailed solution for the region 1

160 The phenomenon in this region of the cuboid is well  
161 known case of the convective heat transfer from down-  
162 faced horizontal plate. For the case of rectangles (Fig. 3  
163 the cross-section B-B) streamlines are parallel to each  
164 other. The boundary layer arises from the axes of sym-  
165 metry and diagonals of the surface. According to the  
166 patterns of the stream lines shown on the dawn faced  
167 horizontal rectangular plate view (Fig. 3 B-B), one can  
168 distinguished two sub regions: first, with two rectangles  
169 (1l) and the second one, with eight triangles (1c). For the  
170 first of them the control surface  $A$  has the same width  
171 independently on the position along the boundary layer  
172 on the plate. For the triangles (1c) the width of the  
173 control surfaces  $A$  are the function of not only the  
174 thickness of boundary layer ( $\delta$ ) but also the distance  
175 from the edges.

#### 176 2.1.1. Bottom lateral side

177 For the rectangles the control surfaces can be defined  
178 as (Fig. 3 B-B):

$$A_{1l} = (b - a) \delta_{1l} \quad \text{and} \quad dS_{1l} = (b - a) dx \quad (14)$$

180 and from the mean velocity of the fluid flow along the  
181 streamlines (6) is:

$$\bar{w}_x = \frac{1}{\delta_{1l}} \int_0^{\delta_{1l}} w_x dy = \frac{g\beta\Delta T \delta_{1l}^2}{72\nu} \frac{d\delta_{1l}}{dx} \quad (15)$$

183 Substituting (14) and (15) into (13) one obtain  
184 equation:

$$3\delta_{1l}^3 \left( \frac{d\delta_{1l}}{dx} \right)^2 + \delta_{1l}^4 \frac{d^2\delta_{1l}}{dx^2} = \frac{432 \left( \frac{a}{2} \right)^3}{Ra_{a/2}} \quad (16)$$

186 where

$$Ra_{a/2} = \frac{g\beta\Delta T \left( \frac{a}{2} \right)^3}{\nu a} \quad (17)$$

188 Eq. (16) has the solution in the form of boundary  
189 layer thickness:

$$\delta_{1l} = \frac{4.478 \left( \frac{a}{2} \right)^{3/5} x^{2/5}}{Ra_{a/2}^{1/5}} \quad (18)$$

and next, according to the Eq. (12), one can calculate the  
mean value of the heat transfer coefficient for this re-  
gion:

$$\bar{\alpha}_{1l} = \frac{2}{a} \int_0^{a/2} \frac{2\lambda}{\delta_{1l}} dx = 0.744\lambda \frac{Ra_{a/2}^{1/5}}{a/2} \quad (19)$$

#### 2.1.2. Bottom corner side

195 The streamlines below the defined above triangular  
196 corner's regions (1c) are directed perpendicularly to the  
197 edges of the plate along the  $x$  or  $z$ -coordinate (Fig. 3 "B-  
198 B"). The velocity of the fluid  $w_x$  and  $w_z$  is described by  
199 the same function due to symmetry of the phenomenon.  
200

The control surfaces for these rectangular triangles  
201 are defined as:  
202

$$A_{1c} = z \delta_{1c} \quad \text{and} \quad dS_{1c} = z dx \quad (20)$$

and the mean velocity value obtained from (6) is: 204

$$\bar{w}_x = \frac{g\beta\Delta T \delta_{1c}^2}{72\nu} \frac{d\delta_{1c}}{dx} \quad (21)$$

Writing the Eq. (13) for this surfaces in the form: 206

$$\frac{1}{6} \frac{\rho c_p \delta_{1c}}{\lambda} d(A_{1c} \bar{w}_x) = dS_{1c} \quad (22)$$

and 208

$$\frac{1}{432} \frac{Ra_{a/2}^{1/5}}{\left( \frac{a}{2} \right)^3} \delta_{1c} \frac{d}{dx} \left( \delta_{1c} \frac{d\delta_{1c}}{dx} \right) = 1 \quad (23)$$

one can find the solution: 210

$$\delta_{1c} = \frac{4.478 \left( \frac{a}{2} \right)^{3/5} x^{2/5}}{Ra_{a/2}^{1/5}} \quad (24)$$

212 In this subregion the fluid flow starts from the hy-  
213 potenuse of each rectangular triangle and goes perpen-  
214 dicularly to the edges so the length of boundary layer  
215 along streamlines can be described by: ( $x' = (a/2) - x$ )  
216 (Fig. 4) which changes from  $x' = a/2$  for  $z = 0$  to  $x' = 0$   
217 for  $z = a/2$ . Taking it into account in Eq. (24) one can  
218 obtain the boundary layer thickness in the form:

$$\delta_{1c} = \frac{4.478 \left( \frac{a}{2} \right)^{3/5} \left( \frac{a}{2} - x \right)^{2/5}}{Ra_{a/2}^{1/5}} \quad (25)$$

and next the mean heat transfer coefficient from this  
220 regions:  
221

$$\bar{\alpha}_{1c} = \frac{1}{S} \int_S \frac{2\lambda}{\delta_{1c}} dS = \frac{16\lambda}{a^2} \frac{Ra_{a/2}^{1/5}}{4.478 \left( \frac{a}{2} \right)^{3/5}} \int_0^{a/2} \int_{((a/2)-z)}^{a/2} \left( \frac{a}{2} - x \right)^{-2/5} dx dz = 0.93\lambda \frac{Ra_{a/2}^{1/5}}{\frac{a}{2}} \quad (26)$$

### 2.2. Solution for the region 2 223

224 The heat transfer in this region can be treated as the  
225 well-known case of natural convection from isothermal  
226 vertical surface. Instead of the typical vertical plates for  
227 the cuboid the boundary layer thickness is not equal  
228 zero at the bottom edge but is equal to the final

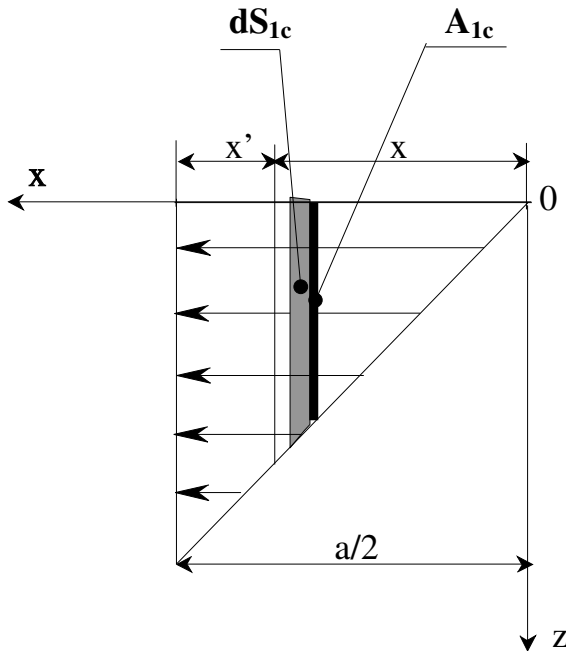


Fig. 4. Enlarged fragment of the presented on Fig. 3 B-B the bottom corner subregion (1c) with the explanation of fluid flow model and control surfaces definitions.

boundary layers thickness from the previous subregion ( $\delta_{1lf}$ ) or ( $\delta_{1cf}$ ) (see Figs. 2 and 3 A-A). Because the values of final boundary layers thickness differs from each other this was the reason why the region 2 has been divided into two sub regions: the vertical lateral (2l) and corner (2c) one. For the first of them (2l) the initial values of boundary layer thickness is constant (Eq. (18) for  $x = a/2$ ) but for region (2c) it is the function of the distance from the corner of the cuboid (Eq. (24)).

Both vertical lateral side (2l) and corner side (2c) have the control surfaces defined as:

$$A_{2l} = y\delta_{2l} \quad \text{and} \quad dS_{2l} = y dy \quad (27)$$

and the mean velocity value obtained from (6):

$$\bar{w}_y = \frac{g\beta\Delta T\delta_{2l}^2}{40\nu} \quad (28)$$

Comparing the heat flux emitted by the heated wall with the heat flux transported by the fluid one can obtain the equation:

$$\frac{1}{240} \frac{Ra_c}{c^3} \frac{\delta_{2l}}{y} \frac{d}{dy} (y\delta_{2l}^3) = 1 \quad (29)$$

which solution is the boundary layer thickness

$$\delta_{2l} = \left( \frac{240c^3}{Ra_c} \frac{4}{7} y \right)^{1/4} \quad (30)$$

### 2.2.1. The vertical lateral side 249

For estimating the mean heat transfer coefficient for the subregion (2l) one should take the length of the boundary layer as  $(c + \delta_{1lf})$  and then integrating borders from  $(-\delta_{1lf})$  to  $(c)$ , where ( $\delta_{1lf}$ ) is the final thickness of boundary layer from bottom in lateral region (18) for ( $x = a/2 = \text{const.}$ ), described by equation: 250 251 252 253 254 255

$$\delta_{1lf} = \frac{4.478 \left(\frac{a}{2}\right)^{3/5} \left(\frac{a}{2}\right)^{2/5}}{Ra_{a/2}^{1/5}} = \frac{2.239a}{Ra_{a/2}^{1/5}} \quad (31)$$

Introduction Eq. (30) into (12) leads to the local and next the mean heat transfer coefficient from this region 257 258

$$\bar{\alpha}_{2l} = \frac{2\lambda}{c} \int_{-2.239a/Ra_{a/2}^{1/5}}^c \left( \frac{4}{7} \frac{240c^3}{Ra_c} \right)^{-1/4} y^{-1/4} dy \quad (32)$$

and then 260

$$\bar{\alpha}_{2l} = 0.779\lambda \frac{Ra_c^{1/4}}{c} \left[ 1 + \left( \frac{2.239a}{Ra_{a/2}^{1/5}c} \right)^{3/4} \right] \quad (33)$$

### 2.2.2. The vertical corner region 262

For estimating the mean heat transfer coefficient from the subregion (2c) one should take the length of boundary layer as  $c + \delta_{1cf}$  and then integrating borders from  $(-\delta_{1cf})$  to  $(c)$ , where ( $\delta_{1cf}$ ) is the final thickness of boundary layer from bottom in the corner region. Due to the symmetry of the phenomenon ( $x = z$ ). 263 264 265 266 267 268

Accordingly to Eq. (25) for  $x = a/2$  and  $z' = (a/2) - z$  the final value of the boundary layer thickness for this sub region is: 269 270 271

$$\delta_{1cf}(z) = \frac{4.478 \left(\frac{a}{2} - z\right)^{3/5} \left(\frac{a}{2}\right)^{2/5}}{Ra_{a/2}^{1/5}} \quad (34)$$

The mean heat transfer coefficient from the regions (2c) is described by the equation: 273 274

$$\bar{\alpha}_{2c} = \frac{1}{a/2} \int_0^{a/2} \left[ \frac{1}{c} \int_{-\delta_{1cf}(z)}^c \frac{2\lambda}{\left( \frac{4}{7} \frac{240c^3}{Ra_c} y \right)^{1/4}} dy \right] dz = 0.779\lambda \frac{Ra_c^{1/4}}{c} + 0.984\lambda \frac{Ra_c^{1/4}}{Ra_{a/2}^{3/20}} \frac{a^{3/4}}{c^{7/4}} \quad (35)$$

### 2.3. Solution for the region 3 276

Region 3 is known case of the heat transfer from the horizontal rectangular plate facing upward, for example [22]. The stream lines are shown schematically on Fig. 3 (cross-section C-C). In this region the rectangular plate should also be considered as the sum of two rectangles and eight triangles and the heat transfer is now influ- 277 278 279 280 281 282

283 enced by boundary layer formed on the bottom and next  
 284 vertical sides of the cuboid. Integration of the heat  
 285 transfer coefficient has to take into account the final  
 286 boundary layer thickness  $\delta_{2lf}$  and  $\delta_{2cf}$ .

287 2.3.1. The upper lateral region

288 The heat transfer in this region is influenced by the  
 289 final boundary layer thickness from the lateral vertical  
 290 side (2lf). The boundary layer thickness obtained for  
 291 lateral top regions in the form [22]:

$$\delta_{3l} = \frac{4.478 \left(\frac{a}{2}\right)^{3/5} x^{2/5}}{Ra_{a/2}^{1/5}} \quad (36)$$

293 should be now integrated from  $(-\delta_{2lf})$  to  $(a/2)$ , where  
 294 final thickness of boundary layer ( $\delta_{2lf}$ ) can be calculated  
 295 from (30) for  $(y = c + \delta_{1lf})$ :

$$\delta_{2lf} = \delta_{2l}(y = c + \delta_{1lf}) = \left(\frac{4}{7} \frac{240c^3}{Ra_c}\right)^{1/4} \left(c + \frac{2.239a}{Ra_{a/2}^{1/5}}\right)^{1/4} \quad (37)$$

297 Then one can obtain the mean heat transfer coeffi-  
 298 cient:

$$\bar{\alpha}_{3l} = \frac{1}{a/2} \int_{-\delta_{2lf}}^{a/2} \frac{2\lambda}{\delta_{3l}} dx = 0.744\lambda \frac{Ra_{a/2}^{1/5}}{\frac{a}{2}} \left\{ 1 + \frac{\left[\frac{4}{7} \frac{240c^3}{Ra_c} \left(c + \frac{2.239a}{Ra_{a/2}^{1/5}}\right)\right]^{3/20}}{\left(\frac{a}{2}\right)^{3/5}} \right\} \quad (38)$$

300 2.3.2. The upper corner region

301 The final boundary layer thickness from (2cf) subre-  
 302 gion is the function of coordinates  $(x)$  or  $(z)$ , so for the  
 303 upper triangles the Eq. (37) should be transformed as (34)  
 304 to:

$$\delta_{2cf} = \delta_{2c}(y = c + \delta_{1cf}) = \left(\frac{4}{7} \frac{240c^3}{Ra_c}\right)^{1/4} \left(c + \frac{4.478 \left(\frac{a}{2} - x\right)^{3/5} \left(\frac{a}{2}\right)^{2/5}}{Ra_{a/2}^{1/5}}\right)^{1/4} \quad (39)$$

306 and the mean value of the heat transfer coefficient for  
 the regions (3c) can be described as:

$$\bar{\alpha}_{3c} = \frac{4}{a^2} \int_{-\delta_{2cf}(x)}^{a/2} \left( \int_{-\delta_{2cf}(z)}^{a/2} \frac{2\lambda}{\delta_{3c}} dx \right) dz = 0.744\lambda \frac{Ra_{a/2}^{1/5}}{a/2} \left[ 1 + \frac{\left(\frac{4}{7} \frac{240c^3}{Ra_c}\right)^{3/20}}{\left(\frac{a}{2}\right)^{3/5}} \left(c + \frac{1.477a}{Ra_{a/2}^{1/5}}\right)^{3/20} \right] \quad (40)$$

where the last integrating in (40) was replaced by the  
 mean value without considerable inaccuracy.

2.4. The Nusselt–Rayleigh relation for the isothermal cuboid

Substituting (19), (26), (32), (34), (37) and (39) to the  
 Eq. (1) the mean heat transfer coefficient for the cube  
 can be estimated. Majority of the heat transfer analyses  
 are based on correlations Nusselt number versus Ray-  
 leigh number in the form:

$$Nu = CRa^n \quad (41)$$

Nusselt and Rayleigh numbers are defined as:

$$Nu_L = \frac{\bar{\alpha}L}{\lambda} \quad \text{and} \quad Ra_L = \frac{g\beta\Delta TL^3}{\nu\alpha} \quad (42)$$

with  $L$  as the characteristic linear dimension.

On the base of our own and other investigators data  
 we have been considered the linear characteristic length  
 choice. We taken into account height of the cuboid  $(c)$ ,  
 the boundary layer length  $(a + c)$ , the square root of the  
 surface  $(\sqrt{A})$  and the length defined by:

$$L = \frac{6V}{F} = \frac{3abc}{ab + ac + bc} \quad (43)$$

where  $V$  is the volume and  $F$  is cuboid's surface,

Ultimately we have chosen the characteristic length  
 (43) and substituting:

$$Ra_{a/2} = Ra_L \left(\frac{ab + ac + bc}{6bc}\right)^3 \quad \text{and} \quad Ra_c = Ra_L \left(\frac{ab + ac + bc}{3ab}\right)^3 \quad (44)$$

the  $Nu_L(Ra_L)$  relation can be described in form:

$$Nu_L = X Ra_L^{1/5} + Y Ra_L^{1/4} \quad (45)$$

where

$$X = \frac{a(6bc)^{2/5}}{4(ab + ac + bc)^{7/5}} \left\{ 2.976b + 0.372a + \frac{1.488}{\left(\frac{a}{2}\right)^{3/5}} \left[\frac{4}{7} \frac{240c^3}{Ra_L \left(\frac{ab+ac+bc}{3ab}\right)^3}\right]^{3/20} \left[ (b - a) \times \left(c + \frac{2.239a}{Ra_L^{1/5} \left(\frac{ab+ac+bc}{6bc}\right)^{3/5}}\right)^{3/20} + a \left(c + \frac{1.477a}{Ra_L^{1/5} \left(\frac{ab+ac+bc}{6bc}\right)^{3/5}}\right)^{3/20} \right] \right\} \quad (46)$$

and

Downloaded from mostwiedzy.pl

MOST WIEDZY

$$Y = \frac{c(3ab)^{1/4}}{2(ab + ac + bc)^{5/4}} \left[ 1.558(a + b) + \frac{3.936a\left(\frac{a}{c}\right)^{3/4} + 1.558(b - a)\left(2.239\frac{a}{c}\right)^{3/4}}{Ra_L^{3/20} \left(\frac{ab+ac+bc}{6bc}\right)^{9/20}} \right] \quad (47)$$

339 The Eq. (45) with coefficients (46) and (47) has the  
340 universal form and does not depend on the cuboids  
341 position—it makes allowance for the influence both the  
342 horizontal and vertical sides of the block, which are  
343 usually described separately with the exponents: 1/5 and  
344 1/4 accordingly.

### 345 3. Experimental apparatus and procedure

346 Experiment was conducted in the air in a vessel with  
347 the volume of 1.5 m<sup>3</sup>. The tested cuboid was made of  
348 polished aluminium and had the dimensions: 0.2, 0.1,  
349 and 0.045 m. It was hanged in the vessel with the use of  
350 two nylon wires which was 0.5 mm thick in three posi-  
351 tions of cuboid's orientation: I-vertical-for height  $c =$   
352 0.2 m, II-lateral-for height  $c = 0.1$  m and III-horizontal-  
353 for height  $c = 0.045$  m.

354 The electric heater (power transistors) was placed  
355 inside the cuboid. Heat flux from the surface of the  
356 block to surrounding test fluid was transferred mainly  
357 by laminar convection and partially by radiation. Six  
358 thermocouples were used to measure the surface tem-  
359 perature, one on the each side of the cube. They were  
360 soldered into holes of aluminium with the tips of about  
361 0.001 m. Four thermocouples were used to measure the  
362 bulk temperature ( $T_\infty$ ) of the fluid (air) at different levels  
363 in the tank. The inaccuracy of the temperature mea-  
364 surement did not exceed  $\pm 0.1$  K. Establishing of differ-  
365 ent steady states was made by a cooling system located  
366 at the top of the vessel. During the experimental runs the  
367 surface temperatures of the cube, bulk temperature of  
368 the fluid and the voltage ( $U$ ) and current of the heater  
369 inside the cuboid ( $I$ ) were measured. All these data were  
370 recorded during established steady states. The time of

obtaining a thermal equilibrium and performing of ex- 371  
perimental studies was about 6 h for one experimental 372  
point. 373

### 4. Experimental results and analysis 374

In steady-state conditions the heat balance at the 375  
exterior surface requires that the rate of heat gain is 376  
equal to the rate of heat loss. This balance must be 377  
maintained between the heat flux form inside the cuboid 378  
and the convective and radiative losses from the external 379  
surfaces to the air. The only source of heat flux form 380  
inside the cube was the electric power of the heater. 381  
Because thin nylon wires eliminated the solid metal 382  
support of the cuboid, the heat losses by conduction 383  
through the support have not been taken into account. 384

A series of experimental runs in air according to the 385  
apparatus described above was made in three configu- 386  
rations of the cube. For every steady-state point the 387  
temperature of the cuboid's sides ( $T_w$ ), the bulk fluid 388  
( $T_\infty$ ) and the electric power of the hater ( $UI$ ) was saved 389  
by computer system. 390

Then the Nu and Rayleigh numbers were estimated 391  
as: 392

$$Nu_L = \frac{\alpha L}{\lambda}, \quad Ra_L = \frac{g\beta(T_w - T_\infty)L^3}{\nu\alpha} \quad (48)$$

where  $\alpha$  was calculated from the Newton's law: 394

$$\alpha = \frac{\dot{Q}_c}{F(T_w - T_\infty)} = \frac{UI - \dot{Q}_r}{F(T_w - T_\infty)} \quad (49)$$

and  $\dot{Q}_r$  is the radiative heat flux form the cuboids sur- 396  
face. 397

All measurements were counted out with the least 398  
square method using three proposed characteristic 399  
lengths. The first one was the height of the cuboid, what 400  
is the equivalent of the characteristic linear dimension 401  
used for the vertical plates. It gave the  $Nu(Ra)$  relation 402  
(Fig. 5): 403

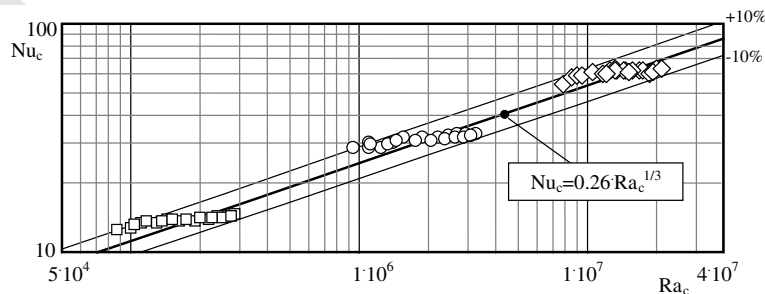


Fig. 5. Experimental results in comparison with theoretical values for three positions of the tested cuboid: (□) position I, (○) position II, (◇) position III in the logarithmic scale with the height of the cuboid as the characteristic linear dimension.



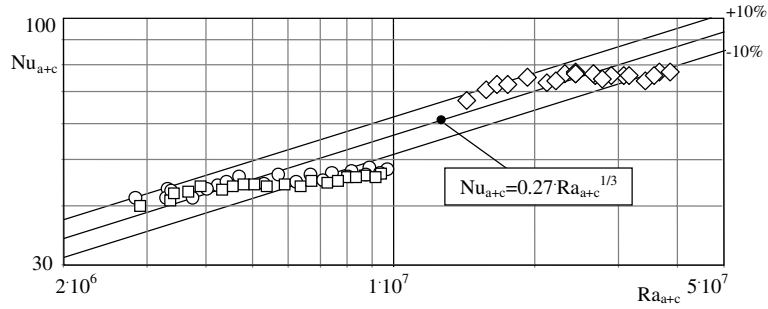


Fig. 6. Experimental results in comparison with theoretical values for three positions of the tested cuboid: (□) position I, (○) position II, (◇) position III in the logarithmic scale with the sum of height and length of the cuboid as the characteristic linear dimension.

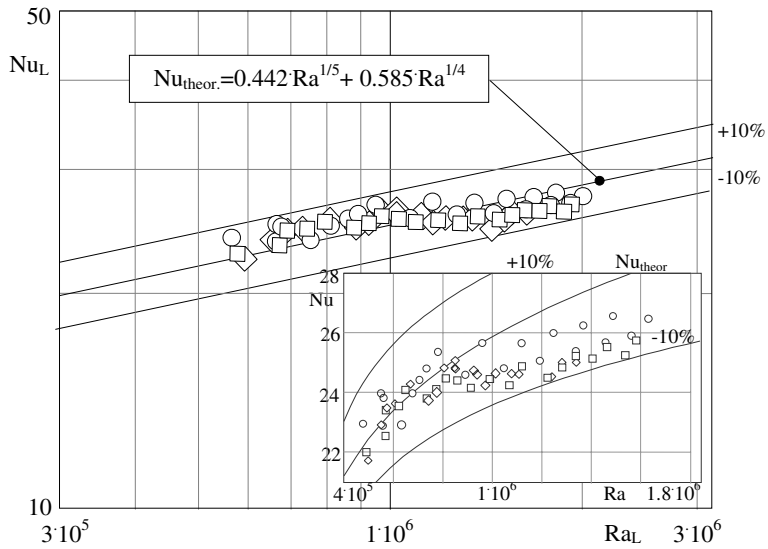


Fig. 7. Experimental results in comparison with theoretical values for three positions of the tested cuboid: (□) position I, (○) position II, (◇) position III in the logarithmic scale with enlarged detail in non-logarithmic scale.

$$Nu_c = 0.26 Ra_c^{1/3} \tag{50}$$

$$Nu_L = 0.442 Ra_L^{1/5} + 0.585 Ra_L^{1/4} \tag{53}$$

The second linear dimension was the length of the boundary layer, equal the sum of the length and height of the cuboid  $(a/2 + c + a/2)$ . Then obtained criterial relation was similar to (50) (Fig. 6):

what is adequate to: 419

$$Nu_{a+c} = 0.27 Ra_{a+c}^{1/3} \tag{51}$$

$$Nu_L = 1.61 Ra_L^{1/5} \text{ or } Nu_L = 0.807 Ra_L^{1/4} \tag{54}$$

that agrees well with (52) within  $\pm 1.35\%$ . 421

Ultimately the characteristic length  $(L = 6V/F)$  (43) turned out the most useful and allowed performing all experimental result, apart from the position of the cuboid (Fig. 7). The obtained relation can be drawn in form

### 5. Conclusions 422

$$Nu_L = 1.596 Ra_L^{1/5} \text{ or } Nu_L = 0.818 Ra_L^{1/4} \tag{52}$$

The natural convection heat transfer in unlimited space from isothermal cuboid has been theoretically and experimentally investigated. Obtained correlation  $Nu_L(Ra_L)$  allows calculating the convective heat transfer intensity for the cuboids with any dimensions and positions regarding the direction of gravity acceleration. The solutions are in good agreement with experimental re- 423  
424  
425  
426  
427  
428  
429

For the tested cuboid the  $Nu_l(Ra_l)$  relations, obtained from (45) with (46) and (47) are:

430 sults presented in this paper and would be included into  
431 prepare energy balance objects in the form of cuboid.

#### 432 References

- 433 [1] T. Fujii, H. Imura, Natural-convection heat transfer from  
434 a plate with arbitrary inclination, *Int. J. Heat Mass*  
435 *Transfer* 15 (1972) 755–767.
- 436 [2] F. Restrepo, L.R. Glicksman, The effect of edge conditions  
437 on natural convection from a horizontal plate, *Int. J. Heat*  
438 *Mass Transfer* 17 (1974) 135–142.
- 439 [3] I.P. Warneford, D.E. Fussey, Natural convection from a  
440 constant-heat-flux inclined flat plate, in: *Fifth International*  
441 *Heat Transfer Conference*, 1974.
- 442 [4] J.V. Clifton, A.J. Chapman, Natural-convection on a  
443 finite-size horizontal plate, *Int. J. Heat Mass Transfer* 12  
444 (1969) 1573–1584.
- 445 [5] S.N. Singh, R.C. Birkebak, R.M. Drake Jr., Laminar free  
446 convection heat transfer from downward-facing horizontal  
447 surfaces of finite dimensions, *Prog. Heat Mass Transfer* 2  
448 (1969) 87–98, according to R.E. Faw and T.A. Dullforce.
- 449 [6] T. Schulenberg, Natural convection heat transfer below  
450 downward-facing horizontal surfaces, *Int. J. Heat Mass*  
451 *Transfer* 28 (1985) 467–477.
- 452 [7] D.E. Fussey, I.P. Warneford, Free convection from a  
453 downward facing inclined plate, *Int. J. Heat Mass Transfer*  
454 21 (1978) 119–126.
- 455 [8] T. Fujii, H. Honda, I. Morioka, A theoretical study of  
456 natural convection heat transfer from downward-facing  
457 horizontal surfaces with uniform heat flux, *Int. J. Heat*  
458 *Mass Transfer* 16 (1973) 611–627.
- 459 [9] T. Aihara, Y. Yamada, S. Endo, Free convection along the  
460 downward-facing surface of a heated horizontal plate, *Int.*  
461 *J. Heat Mass Transfer* 15 (1972) 2535–2549.
- 462 [10] T. Schulenberg, Natural convection heat transfer to liquid  
463 metals below downward facing horizontal surfaces, *Int. J.*  
464 *Heat Mass Transfer* 27 (1984) 433–441.
- [11] E. Radziemska, W.M. Lewandowski, Heat transfer by  
natural convection from isothermal downward-facing hor-  
zontal round plate, *Appl. Energy* 68 (2001) 347–366.
- [12] W.M. Lewandowski, E. Radziemska, Free convective heat  
transfer from isothermal vertical round plate, *Appl. Energy*  
68 (2001) 347–366.
- [13] J.R. Culham, M.M. Yovanovich, P. Teertstra, C.-S. Wang,  
Simplified analytical models for forced convection heat  
transfer from cuboids of arbitrary shape, *EEP-Vol. 26-1*,  
*Advances in Electronic Packaging*, vol. 1, ASME, 1999.
- [14] D.J. Cha, S.S. Cha, Three-dimensional natural convective  
flow around two interacting isothermal cubes, *Int. J. Heat*  
*Mass Transfer* 38 (13) (1995) 2343–2352.
- [15] M.M., Yovanovich, Compact models for conductive and  
convective heat transfer in microelectronic applications for  
the new millenium, in: *34th National Heat Transfer*  
*Conference*, August 2000.
- [16] E.R. Meinders, T.H. van der Meer, K. Hanjalič, Local heat  
transfer from an array of wall-mounted cubes, *Int. J. Heat*  
*Mass Transfer* 41 (2) (1998) 335–346.
- [17] H. Nakamura, T. Igaroshi, T. Tsutsui, Local heat transfer  
around a wall-mounted cube in the turbulent boundary  
layer, *Int. J. Heat Mass Transfer* 44 (2001) 3385–3395.
- [18] J.R. Culham, M.M. Yovanovich, S. Lee, Thermally  
modeling isothermal cuboids and rectangular sinks cooled  
by natural convection, *IEEE Trans. Components, Packa-*  
*ging Manuf. Technol., Part A* 18 (3) (1995).
- [19] H.B. Squire, in: S. Goldstein (Ed.), *Modern Developments*  
*in Fluid Dynamics*, Oxford Clarendon Press, 1938, or in  
New York, Dover 1965.
- [20] E.R.G. Eckert, *Heat and Mass Transfer*, Mc. Graw-Hill  
Book Company, New York, 1959, p. 312.
- [21] W.M. Lewandowski, Natural convection heat transfer  
from plates of finite dimensions, *Int. J. Heat and Mass*  
*Transfer* 34 (3) (1991) 875–885.
- [22] W.M. Lewandowski, E. Radziemska, M. Buzuk, H.  
Bieszk, Free convection heat transfer and fluid flow  
structures above horizontal rectangular plates, *Appl.*  
*Energy* 66 (2000) 177–197.

